DECISION SUPPORT SYSTEM FOR BONE FRACTURE DETECTION USING IMAGE PROCESSING TECHNIQUES

Author

NAJWA FAROOQ

Registration Number

Fall 2015-BMS-00000119541

Supervisor

DR. SYED OMER GILANI

DEPARTMENT OF BIOMEDICAL ENGINEERING & SCIENCES

SCHOOL OF MECHANICAL & MANUFACTURING ENGINEERING

NATIONAL UNIVERSITY OF SCIENCES AND TECHNOLOGY,

ISLAMABAD

DECEMBER, 2018

DECISION SUPPORT SYSTEM FOR BONE FRACTURE DETECTION USING IMAGE PROCESSING TECHNIQUES

Author

NAJWA FAROOQ

Registration Number

Fall 2015-BMS-00000119541

A thesis submitted in partial fulfillment of the requirements for the degree of

MS Biomedical Sciences

Thesis Supervisor:

Dr. Syed Omer Gilani

Thesis Supervisor's Signature:_____

DEPARTMENT OF BIOMEDICAL ENGINEERING & SCIENCES

SCHOOL OF MECHANICAL & MANUFACTURING ENGINEERING

NATIONAL UNIVERSITY OF SCIENCES AND TECHNOLOGY,

ISLAMABAD

DECEMBER, 2018

Thesis Acceptance Certificate

It is certified that the final copy of MS Thesis written by Najwa Farooq (Registration No. Fall 2015-BMS-00000119541), of SMME (School of Mechanical & Manufacturing Engineering) has been vetted by undersigned, found complete in all respects as per NUST statutes / regulations, is free of plagiarism, errors and mistakes and is accepted as partial fulfilment for award of MS/MPhil Degree. It is further certified that necessary amendmentsas pointed out by GEC members of the scholar have also been incorporated in thisdissertation.

Signature: _____

Name of Supervisor: Dr. Syed Omer Gilani

Date: _____

Signature (HOD): _____

Date: _____

Signature (Principal): _____

Date: _____

EXAMINATION COMMITTEE

We hereby recommend that the dissertation prepared under our supervision by: Najwa Farooq, Fall 2015-BMS-00000119541. Titled: "DECISION SUPPORT SYSTEM FOR BONE FRACTURE DETECTION USING IMAGE PROCESSING TECHNIQUES" be accepted in partial fulfillment of the requirements for the award of Masters of Science in Biomedical Sciences degree with (___ grade).

Committee Member: Dr. Mohsin Jamil, Assistan Professor, DME, SMME	Dated:
Committee Member: Dr. AsimWaris, Assistant Professor. BMES SMME	Dated:
Committee Member: Dr. MurtazaNajabat Ali, Assiatant Professor, BMES SMME	Dated:
Supervisor: Dr. Syed Omer Gilani, Assistant Professor, BMES SMME	Dated:

_____ _____

Head of Department Date

COUNTERSIGNED

_____ _____

Principal/Dean Date

Declaration

I certify that this research work titled *"Decision Support System for Bone Fracture Detection Using Image Processing Techniques"* is my own work. The work has not been presented elsewhere for assessment. The material that has been used from other sources it has been properly acknowledged / referred.

_____

NAJWA FAROOQ

Fall 2015-BMS-00000119541

Plagiarism Certificate (Turnitin Report)

This thesis has been checked for Plagiarism. Turnitin report endorsed by Supervisor is attached.

_____

Signature of Student

NAJWA FAROOQ

Fall 2015-BMS-00000119541

_____

Signature of Supervisor

Dr. Syed Omer Gilani

Language Correctness Certificate

This thesis has been read by an English expert and is free of typing, syntax, semantic, grammatical and spelling mistakes. Thesis is also according to the format given by the university.

AUTHOR:

_____

NAJWA FAROOQ

Fall 2015-BMS-00000119541

SUPERVISOR:

_____

DR. SYED OMER GILANI

Copyright Statement

Acknowledgement

In the name of ALLAH, the inspirer of truth. All praise and gratitude is to almighty "ALLAH" Who provided ease on my way, and gave me will, strength and health to accomplish this research, Who gave me the power to do, the right to observe and mind to think, judge and analyze.I bow before my compassionate endowments to HOLY PROPHET MUHAMMAD (S. A. W.) who is a torch of guidance for all mankind.

I would like to take the opportunity to thank those people who spent their time and shared their knowledge for helping me to complete my thesis with the best possible results.

I deem it as my utmost pleasure to avail this opportunity to express the heartiest gratitude and deep sense of obligation to my reverend supervisor, Dr. Syed Omer Gilani, Assistant Professor, Department of BMES & R&AI, SMME, NUST, for his keen interest, valuable guidance, enlightened views, worthy suggestions, constructive criticism and inspiring attitude during my studies, research project, and writing of this manuscript.

I would be honored to gratefully acknowledgeMr. AzmatUllahfor his valuable knowledge, encouragement and moral support during my research.

I feel highly obliged in paying my deepest and sincerest gratitude to Dr. Shazia F. Khan (HOD, Radiology, PIMS, Islamabad). I pay my thanks to the staff at Department of Radiology, PIMS, Islamabad, my students Mr. LaraibHasan and Miss TahreemShahid.

Special thanks to my Brother and Sister for their understanding, great cooperation, encouragement and support when it required most.

I pay my humble gratitude to Ms. Areena Khan, my senior and colleague whose support had always been the greatest help in every situation.

Finally, with love and affection, I am forever indebted to my Parents, whom prayers and efforts made me what I am today.

IDEDICATETHIS HUMBLE EFFORTTOMY PARENTS

(May Allah Bless Them)

Abstract

Computer Aided Diagnosis (CAD) has been a major research subject for diagnosing pathologies using computer vision and artificial intelligence. Human body is composed of 206 long, short and irregular bones. Bones are very prone to common pathology known as fractures. There are several etiologies of bone fractures. The bone fractures are of various types ranging from highly devastating comminuted fractures to hair line fractures. An algorithm has been proposed in this study to detect bone fractures using image processing techniques. For that purpose, MATLAB v. R2015a was used to execute the said task. 126 plain radiographic X ray images, acquired from a public sector hospital of Islamabad, containing long bone fractures were classified into "ground truth annotated" and their counterpart "test" data sets. The "test" images were preprocessed by contrast adjustment and noise removal followed by segmentation into background and foreground by Active Contour Model. Hough transform is applied, as a feature extraction technique, after that, for detecting vertical lines in the image which lead to identification of bone fractures. The results were calculated through Jaccard Index and finally the mean precision value for each image was calculated. The percentage precision was equal to 88.52% which is highest or equal to any bone fracture detection algorithm proposed so far up to best of our knowledge. The proposed algorithm open new grounds for CAD analysis of bone fractures, reducing the load of radiology departments of public sector hospitals.

Keywords: CAD, Bone, Fracture, Active Contour Model, Radiograph, Hough Transform, Segmentation, Feature Extraction.

Table of Contents

List of Tables

List of Figures

List of Acronyms

ACM	Active Contour Model
MPV	Mean Precision Value
MRI	Magnetic Resonance Imaging
CT	Computed Tomography
US	Ultrasound

CHAPTER 1: INTRODUCTION

1.1 BACKGROUND

The bone fractures, specially the occult ones, can be missed due to human error particularly in busy public sector hospitals where patient load is more than private setups per day in Department of Radiology. The objective of this study is to develop an Algorithm that can be robust enough to automatically detect bone fractures with high accuracy and precision, through image processing techniques, which would ultimately help to identify fracture in the particular region of the bone.

1.1.1 Anatomy of Bone

The human bone is tough, resilient and high stress and strain bearing body structure, whichprovides site for articulation for various other bones to form movable and immovable joints.Bones also serves as the site for attachment of skeletal muscles. The normal adult humanskeleton contains 206 bones. The typical long bone is grossly divided into three regions;the epiphysis, which is the broad joint forming part of the bone, the metaphysis, which is thenarrow growth plate containing part of the bone and the diaphysis or the shaft of the bone.Short bones usually do not contain these parts specifically(Marieb & Hoehn, 2007).

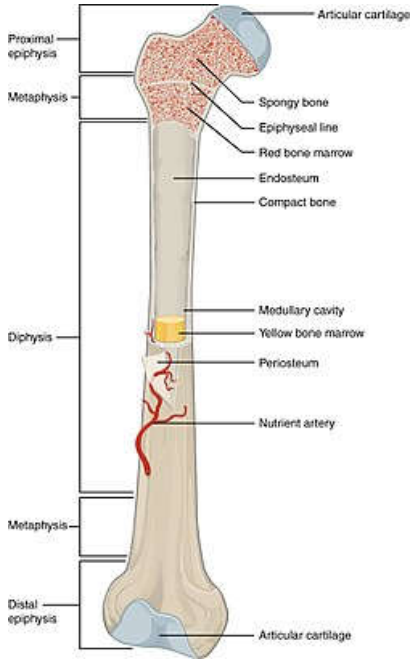

Figure 1: Anatomy of Bone

Bone is a dense connective tissue which is derived embryonically from mesoderm. It ismade up of an outer tough and hard cortical and inner soft and spongy medullary portion. It iscomposed of an outer periosteum and inner highly vascularized endosteum. The periosteum isfurther composed of fibrous and cellular layers. The endosteum lines the medullary cavity ofthe bone. The medullary cavity is composed of bone marrow and matrix made up of mainlyhydroxyapatite, calcium carbonate and collagen fibers. It is the bone marrow where thesynthesis and maturation of red and white blood cells take place(Rizzo, 2015).

At the articulation site (epiphysis), the typical bone is line with articular cartilage to providefriction free movement at the joint. The bones are held together in place by ligaments. Themuscles are attached to the bone by tendons. Together this assembly provide mobility at thejoint.The bone serves as the locomotor, blood cell synthesizing house and protector for visceralorgans by forming skeleton(Netter, Hansen, & Lambert, 2005).

1.1.2 Bone Fracture

The medical condition which leads to loss of continuity in the bone is termed as fracture. Certain bone fractures are treated as a medical emergency. Fracture can be either traumatic, pathological or peri-prosthetic. Fracture results in disruption of periosteum or both periosteumand endosteum, the peri-fracture tissue edema, skin erythema and intense pain.

The major types of fractures are;

a. Closed Fracture

The closed fracture is the type of fracture that does not lead to the fracture endsbreaching the skin barrier. The fracture ends remain inside the body.

b. Open Fracture

The open fracture is the type of fracture which causes one of the fracture ends to breachthe skin barrier and become in contact with the body's external environment(Katherine, 2013).

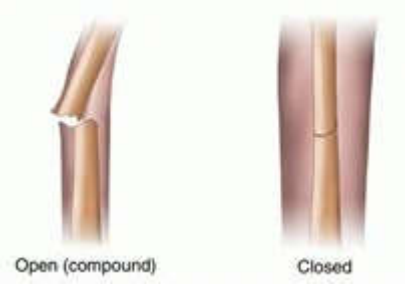

Figure 2: Open vs. Closed Fracture

On the basis of shape, the fracture can be classified as given in the Table 1.

Table 1: Classification of Bone Fractures(McCance & Huether, 2018; Rizzo, 2015; Seffinger et al., 2003)

S. No.	Name of Fracture	Description	Most commonly affected site
1	Linear or Sagittal Fracture	The fracture line is parallel to the long axis of the bone	Long bones
2	Transverse Fracture	The fracture line is perpendicular to the long axis of the bone	Long and short bones
3	Oblique Fracture	The fracture line is diagonal to the long axis of the bone	Long and short bones
4	Hair Line Fracture	Thin lined fracture line the can appear anywhere on the bone	Skull, long bones and patella
5	Comminuted Fracture	Crushing of bone into several fracture fragments	Skull and patella
6	Spiral Fracture	One of the fracture ends twists upon itself	Long bones
7	Compression Fracture	Pathological compression of the bone into wedge or triangular pyramidal shape	Vertebral bodies
8	Avulsion Fracture	Complete discontinuity of one fragment of the bone which is pulled by the muscle tendon	Calcaneus and other short bones
9	Green Stick	The bending of bone due to non-stress bearing capacity of the bone	Children's long bones
10	Growth Plate Fracture	The fracture of metaphysis which can lead to growth impairment	Children's long bones
11	Pond Fracture	The depression in the bone	Children's skull
12	Diastatic Fracture	The fracture along the suture line of the skull	Skull

13	Basilar Fracture	The fracture of the base of the skull	Skull
14	Stress/Fatigue Fracture	The compression of the bone as the result of stress	Hip bones and calcaneus
15	Insufficiency Fracture	Pathological fracture due to lack of blood supply to the bone	Any bone that loses its blood supply
16	Simple Fracture	The fracture that affects the bone only without causing any damage to surrounding soft tissue structures	Any bone
17	Complex Fracture	The fracture that affects more than one bones at a time along with surrounding soft tissues	Any bone
18	Segmental Fracture	The type of fracture that splits a bone at two separate points resulting in creation of a bone segment	Long bones
19	Wedge/ Butterfly Fracture	The fracture that splits a bone fragment into wedge shaped fragment	Long bones

1.1.3 Diagnosis of Bone Fracture

The bone fractures can be detected clinically. The pathological fractures can beprovisionally diagnosed by evaluating the patient's history, which may includeosteoporosis, arthritis, bone tumors or osteogenesisimperfecta. There will be peri-fracturesoft tissue swelling, erythema, and severe pain at the fracture site. The traumaticfractures can also be detected clinically in the same way. The history in the case oftraumatic fractures may include fall, road side or vehicle accident. The peri-prostheticfractures are caused by either varus alignment of the implant or bone resorption as the resultof inflammation at the implant site. The varus alignment of implant results in fracture ofthe lateral aspect of the bone. The history of the patient is also very useful in formulatingprovisional diagnosis of the peri-prosthetic fracture. The clinical evaluation is onlyhelpful in making the provisional diagnosis of the fracture and does not give the absoluteclue about the fracture. That is why some more advanced technique in fracture detection isrequired(Khurana, 2009).

Radiology is the branch of medicine and physics which uses electromagnetic radiations toaid diagnosis for various pathologies which cannot be visualized otherwise. Plain Radiography

is the primary andefficient method for fracture detection. Plain radiography, since the long time, uses screenfilm combination as the image detector. This conventional radiography method usesphosphor screens to convert x rays to light. This light is detected by the silver halide crystalcontaining radiographic films sandwiched between the screens inside the cassette. Thelatent image is formed on the radiographic film which is then processed in a darkroomwhich takes about one hour. The developed image is the readable image. There is nofilm in the digital radiography, rather the image receptor is a cassette which is containsselenium, cesium iodide or gadolinium oxysulfide as a phosphor instead of screen. X raysare converted into light by these detectors which is converted to digital signals which arethen subjected to thin film detectors or CCDs which lead to the prompt formation of animage. The image does not need any developing chemistry. The conventional or plainradiographic image, once projected, cannot be altered in size, shape, contrast or saturation.The digital radiographs have an edge over conventional radiographs in this regard. Thespatial resolution of conventional plain radiography is much better than the digitalradiography.The images of computed tomography, magnetic resonance imaging and ultrasound arealways acquired in the digital format(Brant & Helms, 2012).

Table 2: Description of Plain Radiography (X Ray) as an Imaging Modality (Bushberg & Boone, 2011)

Physics	**Diagnostic Accuracy**	**Advantages**	**Disadvantages**
Uses X-rays in the range of 20kV to 120kV. The x-rays enter the body and attenuate on the basis of tissue density. Soft tissue allows the x rays to pass through while bones absorb them. The exiting x-rays fall on the image receptor and an image is formed resulting in hyperdense (white) bone and hypodense (grey) soft tissue.	Very high	• Highly improved contrast resolution • Excellent evaluation of small and large fractures • Time efficient • Cost efficient • Gold standard in detection of fractures of long bones • Can provide a guess to analyze bone density	• Uses ionizing radiations • Has comparatively low spatial resolution • Can obsolete minor fractures

CHAPTER 2: LITERATURE REVIEW

2.1 ANGLE DETECTION

The first ever published work on automatic fracture detection is of (Tian et al., 2003). This paper portrays a strategy for measuring the neck-shaft edge of the femur, which is one of the principle indicative decides that specialists use to figure out if a break is available at the femur. Exploratory tests performed on test images affirm that the strategy is precise in measuring neck-shaft point and distinguishing certain sorts of femoral fractures

2.2 GRADIENT ANALYSIS

Taking after the principal endeavor,(Yap et al., n.d.)built up a corresponding strategy for identifying femur breaks by investigating the disturbance of trabecular example at the femoral neck. This was finished by extricating and breaking down the introductions of the trabeculae utilizing Gabor filters. Test comes about demonstrated that this strategy supplemented the neck-shaft edge technique. Consequently, brushing the two techniques enhanced the execution of break location.

(Donnelley & Knowles, 2005)worked on computer aided long bone fracture detection. The author stated that the errand of computer helped crack identification for long bone diaphyses. The author demonstrated that it is conceivable to precisely distinguish cracks in the diaphyseal section of a long bone utilizing a composite measure of the slope that joins the extent and course of data, with line parameters ascertained utilizing an adjusted Hough transform.

2.3 DISCRETE WAVELET TRANSFORM

(Smith, Ward, Cockrell, Ha, & Najarian, 2010)detected fractures of pelvis through computer aided image processing. This paper introduces a break discovery technique for the pelvic ring in light of Discrete Wavelet Transform and limit following connected to windows removed from the ring, as characterized by earlier computerized locale division by means of a deformable Spline/ASM model.

2.4 CLASSIFIERS

(Mahendran & Baboo, 2012)ensembelled the system for fracture detection. In their examination work, combination based classifiers were developed, which extricates highlights from the pictures, utilize these components to prepare and test the classifiers with the end goal of distinguishing cracks in X-Ray scans. The different elements manipulated were Contrast, Homogeneity, Energy, Entropy, Mean, Variance, Standard Deviation, Correlation, Gabor orientation (GO), Markov Random Field (MRF), and intensity gradient direction (IGD). Three classifiers, BPNN, SVM and NB classifiers were utilized. Utilizing these elements and classifiers, three single classifiers and four numerous classifiers were created. Every one of the classifiers were tried vivaciously with the test dataset for assessing the champ blend of classifiers and elements that effectively recognizes breaks in a bone scan. The execution measurements utilized are sensitivity, specificity, positive predictive value, negative predictive value, accuracy and execution time. The trial came about demonstrated that utilization of combination classifiers improves the identification limit and the blend of SVM and BPNN produced the best result.

(Al-Ayyoub & Al-Zghool, 2013)tried to determine the type of long bone fracture. In their work, they introduced a machine learning based framework for programmed location of crack sorts in long bones utilizing x-beam images. A few image processing methods were utilized to evacuate diverse sorts of commotion and to remove noise. In the arrangement and testing stage, SVM classifier was observed to be the most accurate with more than 85% exactness under the 10-overlap cross approval strategy. The author claimed that there were numerous future headings of this work. In the first place, testing the proposed procedure with a bigger dataset would give more certainty to the exactness level it can accomplish. Second, concentrating on different variations of the tended to issue, for example, finding the crack's area, dealing with littler bones, and so forth. At long last, incorporating the proposed method into the product of a x-beam machine and giving it an easy to understand graphical interface would make it exceptionally helpful for instructing and research purposes.

(He, Leow, & Howe, n.d.)proposed to utilize a "various leveled" SVM classifier framework for break identification in femur bones.

(Chai, Wee, Swee, Salleh, & Ariff, 2011)proposed GLCM based strategy is proposed to segment the x-beam picture of the hand and separate the bone districts from the delicate tissue

locales. Author began with preprocessing systems, for example, binary conversion and edge recognition methods.

(Anu, Mallikarjunaswamy, of, & 2015, n.d.)did computer based examination methods for the location of bone crack utilizing X-beam/CT pictures. It begins from the preprocessing to evacuate the commotion also, edge distinguishing by utilizing sobel edge filter. After the segmentation the zone of the crack is ascertained. The strategy has been tried on an arrangement of pictures and results have been assessed in light of GLCM components.

2.5 ADAPTIVE THRESHOLDING

(Bandyopadhyay, …, & 2016, n.d.)had additionally built up a product device that could be advantageously utilized by paramedics or expert specialists. The proposed device first portions the bone locale of an info digital X-beam picture from its encompassing tissue district and after that creates the bone-shape utilizing a versatile thresholding approach. Next, it performs unsupervised rectification of bone-form discontinuities that may have been created as a result of division mistakes, lastly identifies the nearness of crack in the bone. In addition, the technique can likewise restrict the line-of-break for simple representation of the crack, distinguish its introduction, and evaluate the degree of harm in the bone. A few ideas from digital geometry, for example, loose straightness and concavity record were used to right form blemishes, and to distinguish crack areas and sort. Probes a database of a few long-bone digital X-ray scans demonstrate agreeable results.

CHAPTER 3: METHODOLOGY

For the purpose of detecting bone fractures, an algorithm was developed which followed the schema shown in Figure 3. To execute the said task, MATLAB v. R2015a was used.

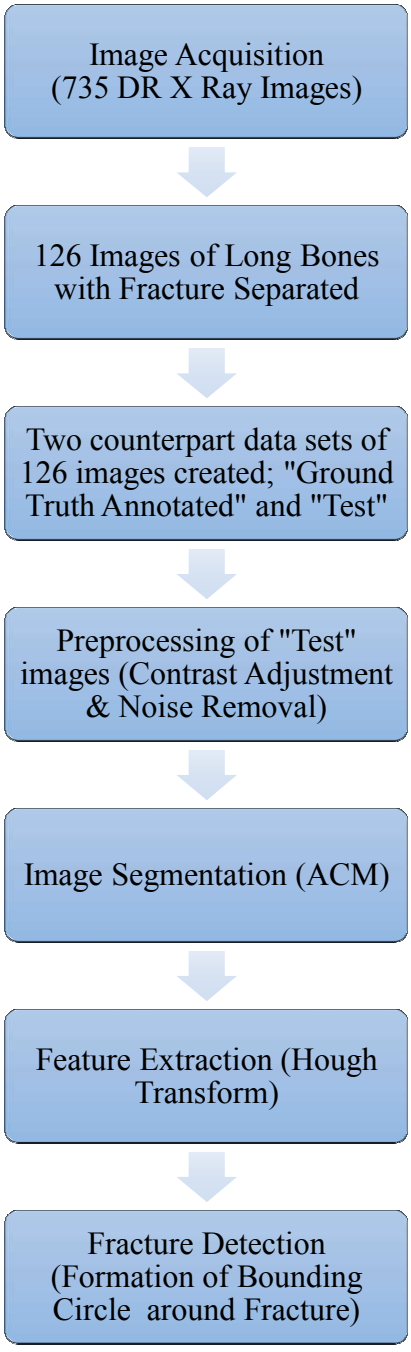

Figure 3: Flow Diagram of the Algorithm Developed for one Fracture Detection

3.1 IMAGE ACQUISITION

For the purpose of the said study, digital plain radiographic images were required. The x ray images were collected from Pakistan Institute of Medical Sciences, Islamabad (PIMS) after the written consent from Head of Department, Radiology. Digital images in DICOM format were acquired. These DICOM images contained both normal and pathological X ray images. The pathological images, containing bone fractures were separated. The total number of images containing bone fractures came out to be 735 from all anatomical areas of the body. These images were converted into JPEG and were cropped to remove patient data. The cropped JPEG images were then sorted and were classified in their respective folders on the basis of the bone affected and area of the bone affected. A data sheet was also created elaborating description of each image.

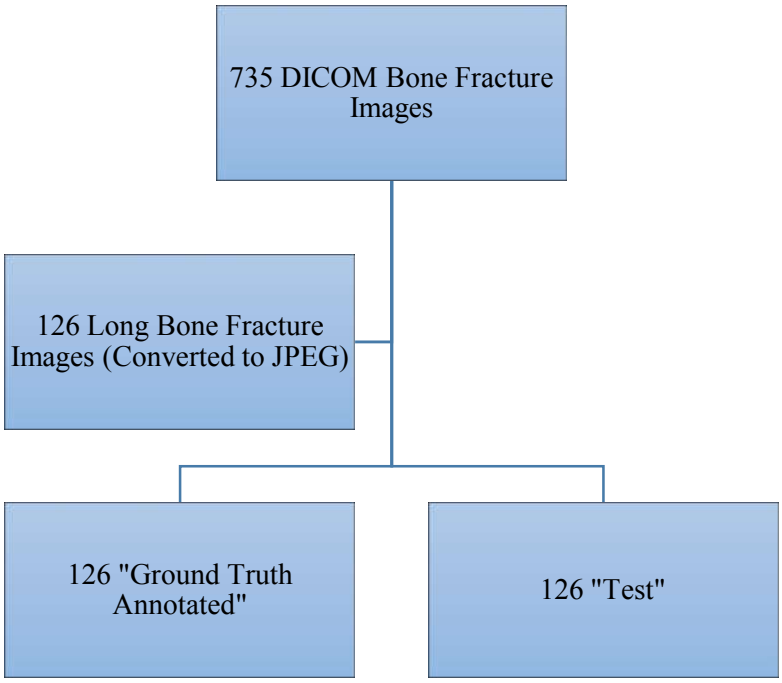

Figure 4: Image Acquisition

Two data sets were created; Ground Truth Annotated and Test. Every image in the Annotated data set was ground truth annotated, manually. The annotation was done by drawing a red square around the fracture area of the bone as shown in Figure 5. In this way, a complete annotated data set of bone fracture images was created. The Test data set was spared as it is.

Figure 5: Ground Truth Annotated Image

The inclusion of 126 images of long bone diaphysis fracture was done from both Test and Annotated data sets. These 126 images were included from humerus, radius, ulna, femur, tibia and fibula.

3.2 PREPROCESSING

3.2.1 RGB to Gray Scale Conversion

The algorithm designed, first reads the JPEG image from the Test data set, which is an RGB. This RGB image is then converted into its weighted sum of red, green and blue components into a Gray Scale 2D image.

3.2.2 Contrast Adjustment

Once the image is converted into gray scale, it is treated by certain contrast enhancement procedures. Background intensity variation was the major problem encountered during. In order to reduce background intensity variation contrast adjustment is performed.

Figure 6: Gray Scale Image after Contrast Adjustment

3.2.3 Morphological Operators

The contrast adjusted images were then morphologically operated. This specific operation was also the part of reducing background intensity variations.

Contrast Adjustment and Morphological Operators resulted in low intensity background, which constitutes surrounding soft tissues, and high intensity foreground, which constitutes the target bone. This approach has facilitated the noise removal and further segmentation technique in a very good manner.

3.2.4 Noise Removal

A low pass filter, Gaussian, was applied on the contrast adjusted image to reduce high frequency signals in the image. The applied Gaussian filter had high sigma value of 2.

This resulted in reduction of fine details, blurring of the edges and image on the whole. But the fine details are not required to be accessed in this study. A fracture usually creates a low intensity area as compared to surrounding bone. This criteria was more than enough to be considered for this study, making contrast resolution to be preferred over spatial resolution of the image. The removal of high intensity signals from the surrounding soft tissue is very important to prepare an image suitable for targeted edge detection and segmentation.

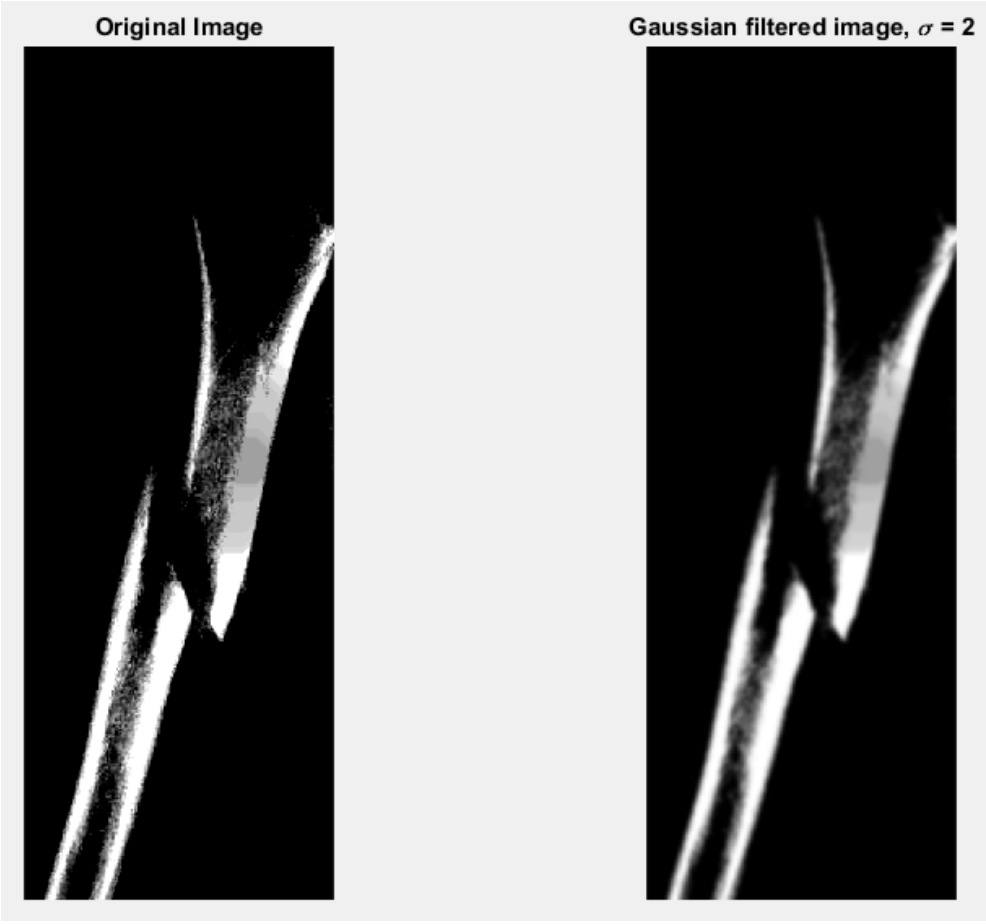

Figure 7: Original Image (Preprocess) vs. Gaussian Filtered Image

3.3 IMAGE SEGMENTATION

After a series of preprocessing operations, the image was prepared to be treated with image segmentation. Image segmentation deals with the breakdown of an image into its useful components. It results in simplification and ease of access to target area of the image over which a specific method is to be applied to extract a particular type of information(Kaur & Kaur, 2014).

For this purpose, Active Contour Model had been used. ACM is also called as snakes or Adaptive thresholding model. It automatically segments the image into background and foreground once the boundaries of foreground are identified.

The image is thought in terms of shape while being segmented by ACM. It begins with drawing one of more curves around the image. The curves drawn move towards the boundary of object of interest with the velocity termed as sine velocity.

A deformable snake is composed of three major components;

I. Set of hinge points "v(s)". These points guide how contour will flow.
II. Internal Elastic Energy. It is the weighted sum of 1st order and 2nd order derivative of v(s). It is the internal energy that controls the deformations of snake. It is composed of Elasticity and Stiffness.
III. External Edge-Based Energy. It depends upon the gradient of the image and image intensity. It is the composite of image energy and constraint energy set by user.

Once the factors for snake has been set, it follows the convergence criteria. The internal and external energies are minimized. The sum of Elasticity, Stiffness and Gradient results in zero. As soon as the sum reaches zero, the boundaries of the target image area are identified(Dhawan, Huang, & Kim, 2008).

MATLAB has an inbuilt command for applying ACM on an image. As mentioned earlier, the gray scale image underwent a chain of preprocessing commands. The preprocessed image was subjected to be segmented by ACM. For that purpose, an initial contour of was specified. A mask of zeros, similar to the size of gray scale image, was created. This mask was modified by creating white pixels of 1 intensity in the middle. The surrounding 25 pixels of each side were left as black or 0 intensity. This resulted in the creation of initial contour location.

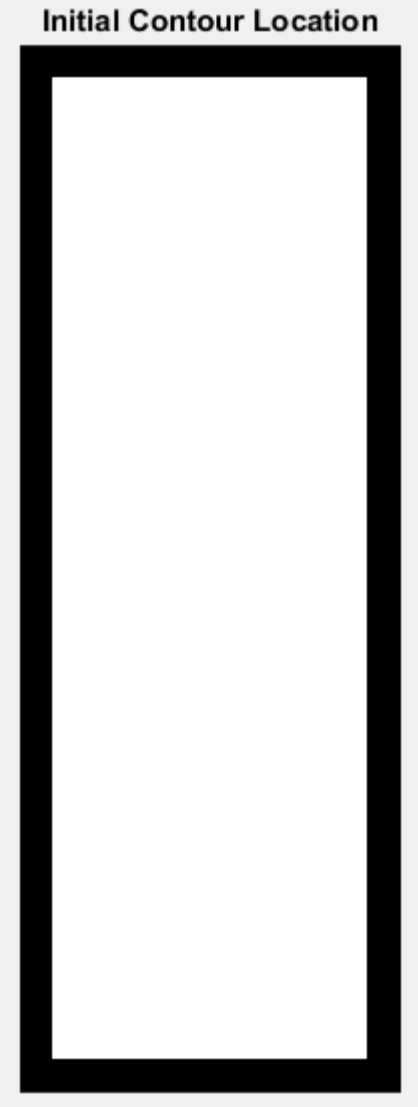

Figure 8: Initial Contour Location

The image was then segmented by using inbuilt MATLAB command to apply active contour model. The mask was convolved over the gray scale image with 300 iterations. The resultant image was perfectly segmented binary image with bone appearing as foreground and soft tissues appearing as background. The segmented out boundaries of the image were also displayed on the gray scale image by finding perimeters in the binary image.

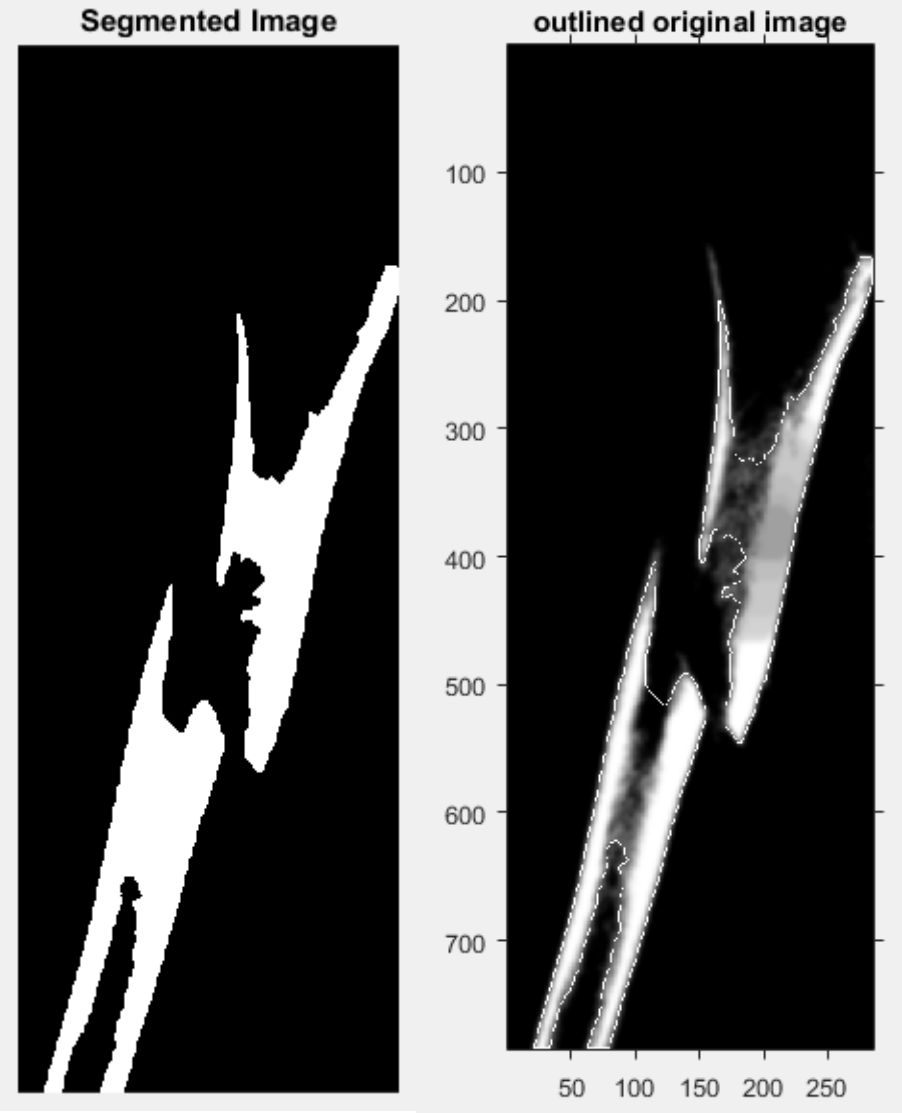

Figure 9: Segmented Image through ACM & Outlined Original Image

3.4 FEATURE EXTRACTION

Feature extraction is the image processing technique meant for extracting a specific feature from the image that could have certain significant importance leading to identification or skimming off relevant required information(Szeliski, 2011).

Hough transform has been used in this study to extract lines from the segmented bone image. Hough transform is a feature extraction technique that identifies lines and certain shapes in an image. The Hough transform is applied over the segmented or edge detected image. Hough

transform extract the vertical lines through voting process in the pixels which are tend to be aligned in the vertically and such pixels are specified through and edge detected image.

A line can be described completely by two quantities, slope and intercept. For this purpose, a parameter space is concocted. This parameter space is the m-c space; where m=slope and c=intercept of the line. A point in x y space in equal to line in parameter space. So, the Hough transform is meant to convert points in x y space to line in m c space. A line can be formed in x y space by two quantities, rho and theta. Rho is the distance perpendicular, normal to the line from the origin (0, 0) and theta is the angle from normal to x axis. This leads to the formation of another space which is termed as Hough space or Rho Theta space. There happens to be sinusoidal lines that corresponds to straight lines in x y plane. Hough space gives the point where sinusoidal curves intersect in a 2D array of accumulator cells where vertical axis specifies distance (rho) and horizontal axis specifies angle (theta). That point specifies the distance (rho) and the angle (theta). Once, rho and theta are identified a straight line can be constructed(Nixon, Aguado, & Elsevier Science Publishers., 2002).

By using MATLAB, standard Hough transform can be computed to detect straight lines in binary image. Two previously described parameters are defined while computing Hough transform through MATLAB; rho resolution and theta resolution. Rho resolution is measured in pixels. It specifies the spacing of Hough transform bins in an accumulator cell along the rho axis. The rho resolution kept in this case is 0.9. Theta is another parameter which is between -90 degrees and +90 degrees. It had been kept between -90 degrees and 89 degrees with an increment of 2 degrees. It specifies the spacing of Hough transform bins along theta axis.

The determination of standard Hough transform is followed by specification of a threshold value. For that purpose, firstly largest elements in each matrix row were identified followed by identification of maximum and minimum values from the identified largest elements in each matrix row. The threshold vale was calculated by:

$$HoughThresh = \left(\frac{(\max(maxHough) - \min(maxHough))}{2}\right) + \min\,(maxHough)$$

Where;

HoughThresh = Hough Threshold

Maxhough = Largest element in each matrix row

The calculated threshold value serves the purpose of taking local maximum in an accumulator array whose values are equal or greater than the fixed threshold value. Threshold value is required to find Hough peaks in an image.

In the next step, Hough peaks were identified. Peaks in the image corresponds to local maxima. The two parameters are determined to identify Hough peaks; minimum peak height, specifies only those values which are higher than the specified value, which is equivalent to threshold value and minimum peak distance, which corresponded to 3, identifies the tallest peak in the signal and ignores all the other peaks with in the minimum peak distance of it. It specifies the distance between the peaks in Hough transform angle detection.

As mentioned earlier, the minimum Hough peak distance used in this case is 3. That corresponds to the angle of the vertical line detected by the Hough transform to be in between 87 and 90 degrees. Any line that has major angle contribution, results in a Hough peak. Hough peak is the landmark for detecting number of bones present in the image. The fracture resulted in low intensities in between high intensity bone area. After significant preprocessing and segmentation, the resultant image constituted of two or more bone fragments depending upon the fracture type. More the bone fragments present, more angle contributions were there in the specified range. If there is no fracture present in the image, there will be only one angle contribution that resulted in single Hough peak. In a pathological case, where bone fracture was present in the image, two Hough peaks were detected as there were two angle contributions present.

A graph was plotted in this context. The middle solid red line constituted Hough threshold. The blue line constituted Hough peaks from maximum Hough transform and red cross were the detected peaks.

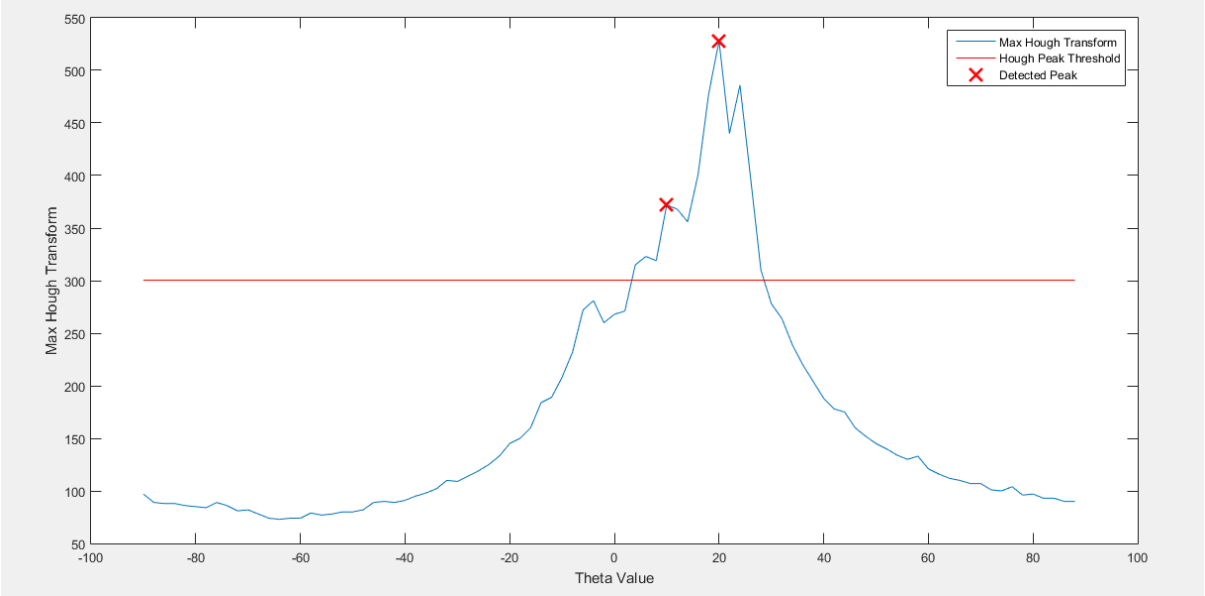

Figure 10: Detected Hough Peaks

In the next step, the site of fracture was located. A filter kernel was created using a flat morphological structuring element termed as strel in MATLAB. Flat structuring element is a logical neighborhood, in which only true pixels are included while calculation. A line shaped structuring element has been used in this case. The line strel has two properties; length and angle. The length is specified by the Hough Convolution Length which is equal to 40 and the angle was specified by Hough peaks calculated earlier. The particular kernel was converted in class double. The kernel was dilated to the amount of 2. This resulted in determination of longest lines in the image. The filter kernel was convolved over the segmented image using imfilter command of MATLAB.

$$imfilter(bw.kern).* bw$$

Where;

imfilter = Inbuilt MATLAB command for filter convolution

bw = Binary image created as the result of segmentation of Gaussian filtered image

kern = A double class filter kernel created from morphologically operated strel line; ultimately dilated to the amount of 2.

The convolution of kernel over the segmented image was followed by calculating the absolute difference between convolved image and gray scale filtered image. Wherever the difference crosses zero within the tolerance of 0.25, it had been determined as the point where fracture exists. Region properties of the image were also determined that included, Area, Major Axis Length, Minor Axis Length, Orientation and Centroid.

A bounding circle is drawn around the area determined as bone fracture on the gray scale image.All of the 126 images upon which the bone fracture has been detected were saved in a folder as “Detected” Images.

Figure 11: Bounding Circle around Fracture Area

CHAPTER 4: RESULTS

4.1 BACKGROUND

Digital X ray images of bone fracture were acquired. 735 images were converted in JPEG format and were annotated manually by creating a square around the fracture area. 126 annotated and non-annotated (test) images were separated. The Test data was treated with the developed algorithm along with the normal images.

4.2 CALCULATION OF RESULTS

The results were calculated using Jaccard Index. It is also known as Intersection over Union technique. Intersection over union is a metric or scale used to find the accuracy of an algorithm that is meant to detect particular object in a particular data set. Two data sets are important for the implementation of Jaccard Index; the "Ground Truth Annotated" data set and the "Detected" data set.

A bounding square was made manually over the fracture area as ground truth in the Annotated data set and a bounding ellipse was created by the algorithm in the Detected data set. The intersection over union metric was applied over all of the 126 images by masking them over each other.

4.3 METHODOLOGY FOR CALCULATING RESULTS

Both the ground truth annotated images and detected images were converted into binary.

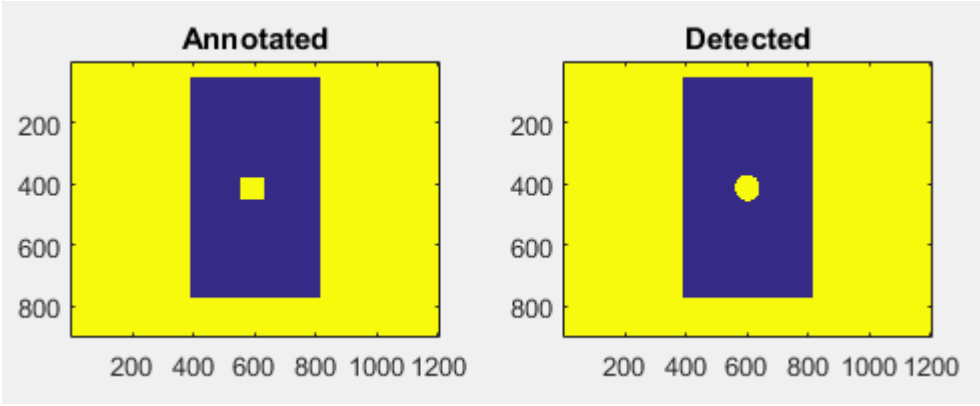

Figure 12: Annotated vs. Detected Binary Images

It was followed by calculation of intersection of the two images.

$$intersectImg = and(gtbw, segbw)$$

Where;

gtbw = binary ground truth annotated image

segbw = binary detected image

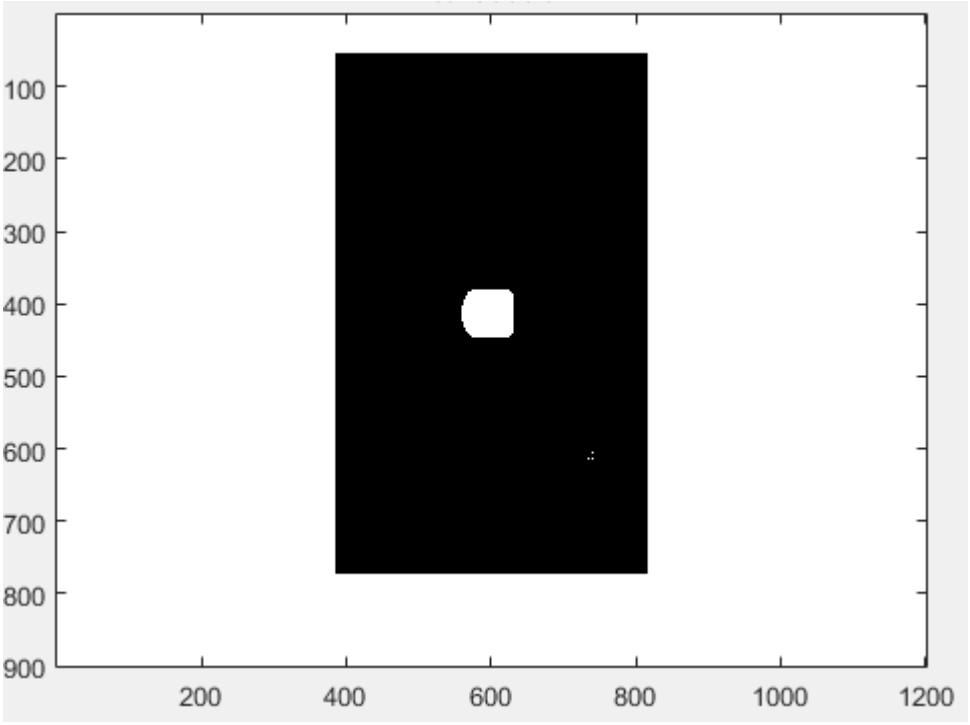

Figure 13: Intersection of two Binary Images

Afterwards, the union of these images was calculated;

$$unionImg = gtbw \mid segbw$$

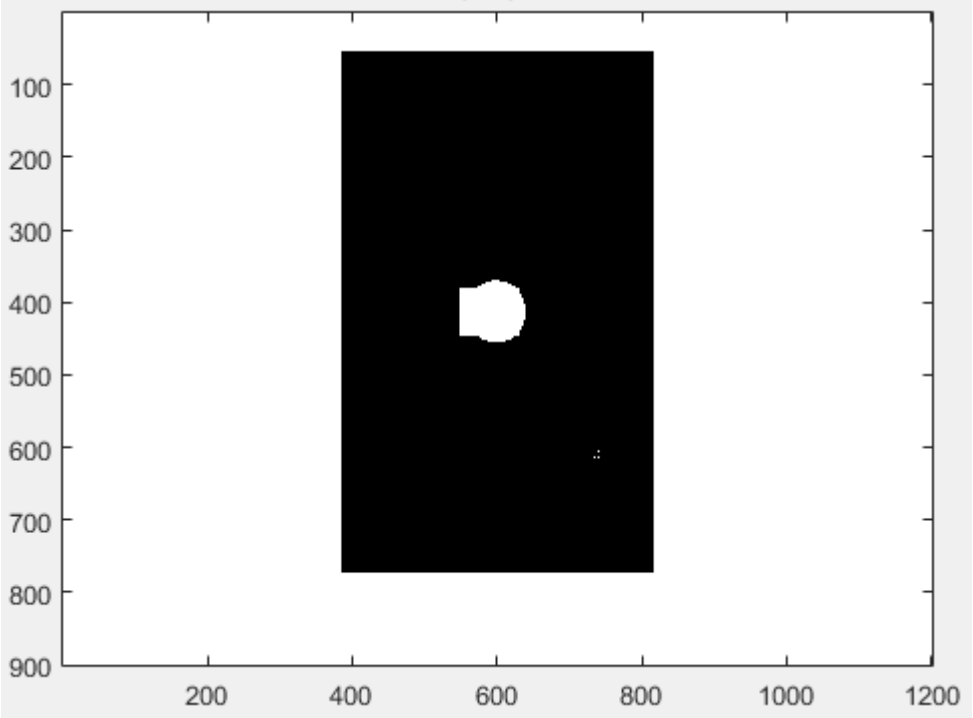

Figure 14: Union of two Binary Images

Two variables; Numerator and Denominator were created by taking the individual sums of intersectImg and unionImg.

$$Numerator = sum(intersectImg(:))$$

$$Denominator = sum(unionImg(:))$$

This lead to the calculation of Jaccard Index by dividing Numerator with Denominator.

$$JaccardIndex = \frac{Numerator}{Denominator}$$

A threshold value ‘t” was determined ranging from 0.5 to 1 with an increment of 0.05. If the Jaccard index calculated falls above 0.5, the intersection over union of masking of annotated and detected images was considered to be a “hit”.

At each threshold value t, a precision value is calculated based on the number of true positives (TP), falsenegatives (FN), and false positives (FP) resulting from comparing the detected fracture area to ground truth fracture area.

$$Precision\ Value = \frac{TP(t)}{(TP(t) + FP(t) + FN(t))}$$

Where;

TP = True Positive

FP = False Positive

FN = False Negative

A true positive is counted when a single predicted object matches a ground truth object with a Jaccard Index abovethe threshold. A false positive indicates a detected fracture had no associated ground truth fracture. A falsenegative indicates an annotated fracture had no associated detected fracture.

The average precision value(MPV) of a single image is then calculated as the mean of the above precision values at each Jaccard Index threshold:

$$MPV = mean(Precision\ Value)$$

4.4 CALCULATED RESULTS

The average precision value or MPV for 126 annotated images masked over the detected images was calculated in MATLAB through Jaccard Index.Jaccard Index for these images varied from 0.9979 to 0.7660The Jaccard Index calculated is shown in the Figure 15:

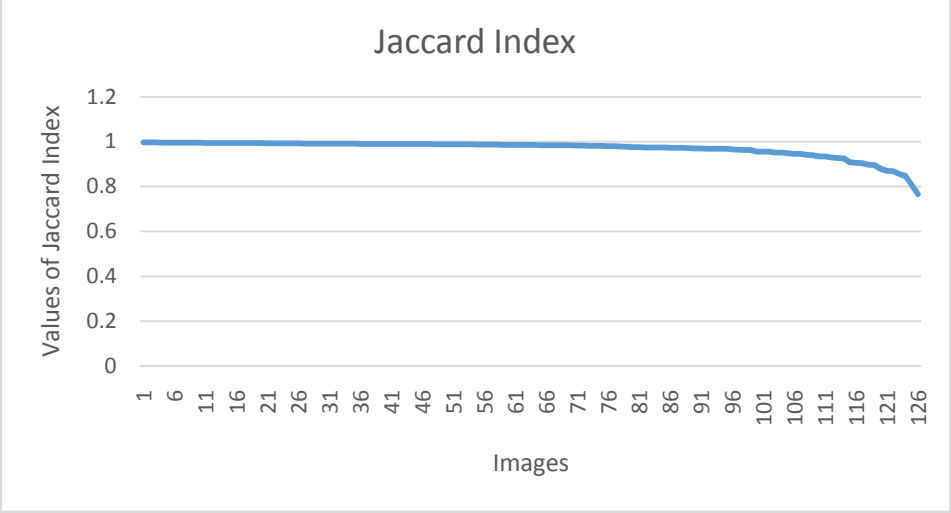

Figure 15: Jaccard Index

The MPV calculated against Jaccard Index, varied from 0.9091 to 0.5455 of every image, is shown in the Figure 16.

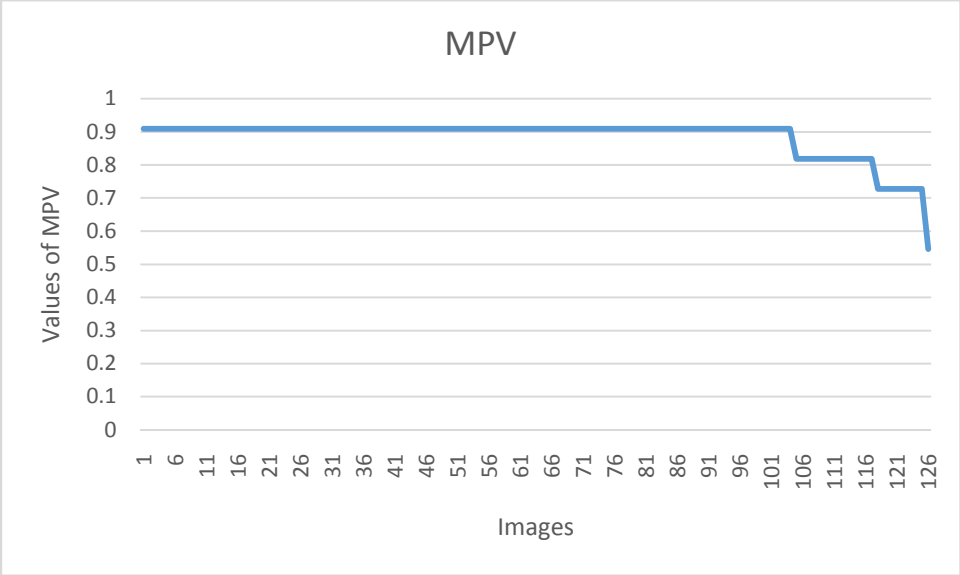

Figure 16: Mean Precision Value

A comparison of JaccardIndex and MPV is illustrated in the Figure 17, below. The illustration clearly shows the similarity in the trend of Jaccard Index and MPV.

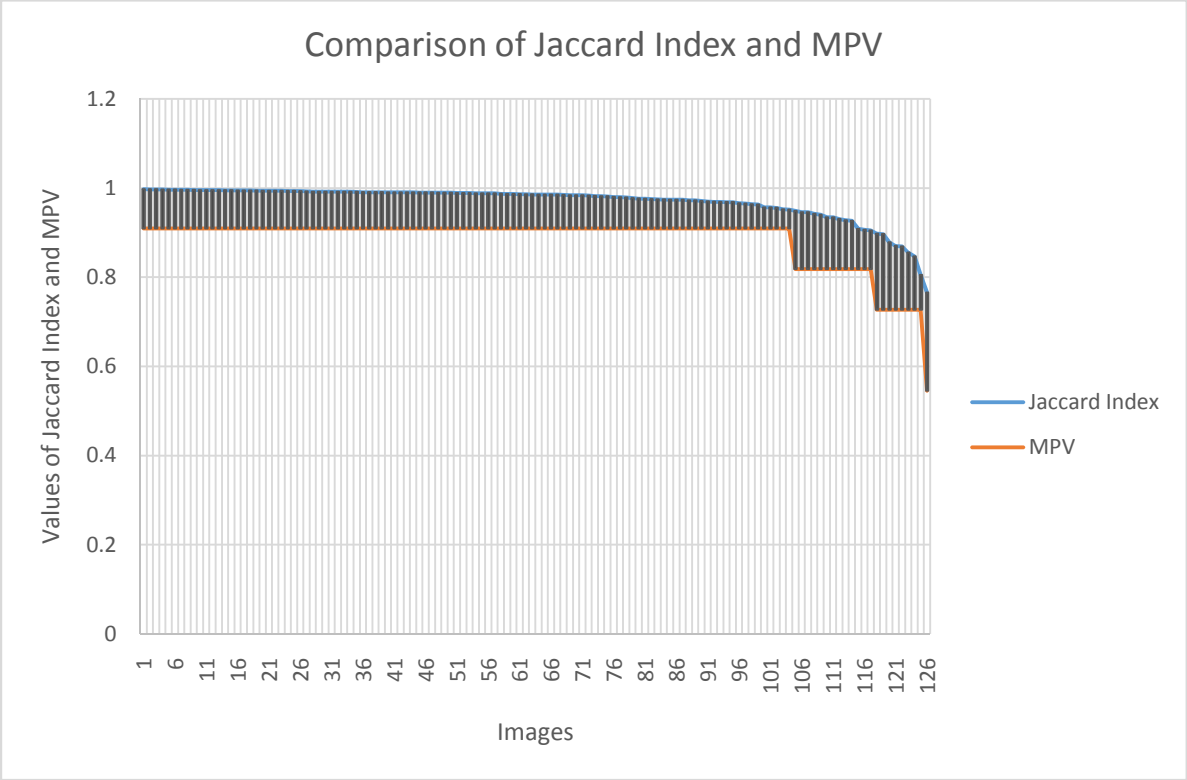

Figure 17: Comparison of Jaccard Index & MPV

The Mean Precision Values calculated for every image were taken into account and percentage of MPVs of 126 images was calculated. The Percentage Precision was 88.52% for 126 x ray images in which bone fractures were detected by the proposed algorithm.

CHAPTER 5: DISCUSSION

An algorithm was developed for automatically detecting the fractures present in the bone. It was composed of preprocessing of the digital X ray images that contained bone fractures followed by image segmentation through Active Contour Model which provided grounds for Hough Transform to work on. Hough Transform was the major feature extraction method used that detected vertical lines in the image and identified the point of break in the bone. These operations were followed by illustrating the results of bone fracture detection by forming a circle around the bone fracture area.

The bones included in the study for testing algorithm were humerus, radius, ulna, femur, tibia and fibula. Orthogonal scans of these bones were included in the study. The bones contained different types of fractures ranging from transverse, spiral, longitudinal, comminuted to hairline. The bone fractures were identified by the developed algorithm and the percentage precision calculated by Jaccard index was equal to 88.52%.

As published by (Donnelley & Knowles, 2005), the bone fractures parallel to the bone edge were missed. Such bone fractures were detected in the proposed algorithm. The bone fractures were detected by training classifiers by(Mahendran & Baboo, 2012). The accuracy of the classifiers ranged from 86.39% to 97.97%. The algorithm developed was successful in detecting 100% of the fractures in the scans but the precision, as stated earlier was 88.52% which is pretty matching the comparative study. The algorithm proposed by(Al-Ayyoub & Al-Zghool, 2013) tested on long bone fracture images had the maximum precision of 88.5% which is equivalent to that of proposed algorithm. The study proposed by (Anu et al., n.d.)used GLCM as a feature extraction technique showed the precision of 76.9% compared to 88.52% of the proposed algorithm. Ismail et al. detected bone fractures in hand through discrete wavelet transform the accuracy of which was 86% which was similar to that of Chai et al. who used GLCM to detect bone fractures.

The proposed algorithm, as discussed previously has comparatively high precision in detecting bone fractures. The algorithm has highly significant clinical implementation in detecting bone fractures by decreasing the load on the department of radiology of public sector

hospitals. The radiologists could get more time to put their expertise in analyzing more complex radiological procedures (MRI, CT and US) than analyzing bone fractures.

The limitations of the algorithm includes:

- The detection of bone fracture in the middle of the shaft of the long bone.
- Non-precision of 11.48%.
- Inability to detect segmented bone fractures

CHAPTER 6: CONCLUSION AND FUTURE RECOMMENDATION

6.1 CONCLUSION

A robust algorithm was developed to automatically detect bone fractures using image processing techniques by combining Active Contour Model as segmentation technique and Hough transform as feature extraction technique. The algorithm was tested o 126 bone fracture images of all fracture types of long bone diaphysis. The results were prepared by calculating Mean Precision Value from Jaccard index or intersection over union criterion. The percentage precision calculated came out to be 88.52% which is either higher of equivalent to the relevant studies. The combination for image segmentation and feature extraction has not been used up till now up to the best of our knowledge.

6.2 FUTURE RECOMMENDATIONS

- Testing the algorithm in the fractures of short bones, skull and vertebrae.
- Testing the algorithm in hospital set up.
- Incorporation of fracture type identification algorithm which can lead to generation to completed medical report regarding the subject matter.

CHAPTER 7: REFERENCES

Al-Ayyoub, M., & Al-Zghool, D. (2013). Determining the type of long bone fractures in x-Ray images. *WSEAS Transactions on Information Science and Applications*, *10*(8), 261–270.

Anu, T., Mallikarjunaswamy, M., of, R. R.-I. J., & 2015, undefined. (n.d.). Detection of bone fracture using image processing methods. *Citeseer*. Retrieved from http://citeseerx.ist.psu.edu/viewdoc/download?doi=10.1.1.739.9543&rep=rep1&type=pdf

Bandyopadhyay, O., … A. B.-C. methods and, & 2016, undefined. (n.d.). Long-bone fracture detection in digital X-ray images based on digital-geometric techniques. *Elsevier*. Retrieved from https://www.sciencedirect.com/science/article/pii/S0169260715002400

Brant, W., & Helms, C. (2012). *Fundamentals of diagnostic radiology*. Retrieved from https://books.google.com.pk/books?hl=en&lr=&id=o_4eoeOinNgC&oi=fnd&pg=PP2&dq=Brant,+William+E+and+Clyde+A+Helms.+Fundamentals+of+Diagnostic+Radiology&ots=mnWcrKw7RA&sig=EW4_XXkvBxMc8pvg7dp45jJ2daA

Bushberg, J., & Boone, J. (2011). *The essential physics of medical imaging*. Retrieved from https://books.google.com.pk/books?hl=en&lr=&id=tqM8IG3f8bsC&oi=fnd&pg=PR1&dq=15.%09Bushberg,+Jerrold+T.+The+Essential+Physics+of+Medical+Imaging.+1st+ed.+Philadelphia:+Lippincott+Williams+%26+Wilkins,+2002.+Print.&ots=9nkx_SjWjo&sig=GP-7jJqIQge8wWZD0u8bnnpaEaY

Chai, H. Y., Wee, L. K., Swee, T. T., Salleh, S., & Ariff, a K. (2011). Gray-Level Co-occurrence Matrix Bone Fracture Detection Center for Biomedical Engineering Biomedical Engineering Group , *8*(1), 26–32. https://doi.org/10.3844/ajassp.2011.26.32

Dhawan, A. P., Huang, H. K., & Kim, D.-S. (2008). *Principles and Advanced Methods in Medical Imaging and Image Analysis*. WORLD SCIENTIFIC. https://doi.org/10.1142/6366

Donnelley, M., & Knowles, G. (2005). where b Y ` b R SUT V c a SUT V qs t r and usv is the width of the line and, 175–178.

He, J. C., Leow, W. K., & Howe, T. Sen. (n.d.). Hierarchical Classifiers for Detection of Fractures in X-Ray Images. In *Computer Analysis of Images and Patterns* (pp. 962–969).

Berlin, Heidelberg: Springer Berlin Heidelberg. https://doi.org/10.1007/978-3-540-74272-2_119

Katherine, A. (2013). *Official CPC Certification Study Guide*. American Medical Association.

Kaur, D., & Kaur, Y. (2014). *International Journal of Computer Science and Mobile Computing Various Image Segmentation Techniques: A Review*. *International Journal of Computer Science and Mobile Computing* (Vol. 3). Retrieved from www.ijcsmc.com

Khurana, J. S. (2009). *Bone pathology*. Humana Press.

Mahendran, S. K., & Baboo, S. S. (2012). Ensemble Systems for Automatic Fracture Detection, *4*(1), 1–4.

Marieb, E. N., & Hoehn, K. (2007). *Human anatomy & physiology*. Pearson Education.

McCance, K. L., & Huether, S. E. (2018). *Pathophysiology-E-Book: The Biologic Basis for Disease in Adults and Children*. Elsevier Health Sciences.

Netter, F. H., Hansen, J. T., & Lambert, D. R. (2005). Netter's clinical anatomy. *2005*, Icon--Learning.

Nixon, M. S., Aguado, A. S., & Elsevier Science Publishers. (2002). *Feature extraction and image processing*. Newnes.

Rizzo, D. C. (2015). *Fundamentals of anatomy and physiology*. Cengage Learning.

Seffinger, M. A., King, H. H., Ward, R. C., Jones, J. M., Rogers, F. J., & Patterson, M. M. (2003). Osteopathic philosophy. *Foundations for Osteopathic Medicine*, *2*, 3–18.

Smith, R., Ward, K., Cockrell, C., Ha, J., & Najarian, K. (2010). DETECTION OF FRACTURE AND QUANTITATIVE ASSESSMENT OF DISPLACEMENT MEASURES IN PELVIC X-RAY IMAGES Dept . Computer Science and VCURES , Virginia Commonwealth University Dept . Emergency Medicine and VCURES , Virginia Commonwealth University. *Emergency Medicine*, 682–685.

Szeliski, R. (2011). *Computer vision : algorithms and applications*. Springer.

Tian, T. P., Chen, Y., Leow, W. K., Hsu, W., Howe, T. Sen, & Png, M. A. (2003). Computing

Neck-Shaft Angle of Femur for X-Ray Fracture Detection (pp. 82–89). https://doi.org/10.1007/978-3-540-45179-2_11

Yap, D., Chen, Y., Leow, W., Howe, T., null, M. P.-, & 2004, undefined. (n.d.). Detecting femur fractures by texture analysis of trabeculae. *Computer.Org*. Retrieved from https://www.computer.org/csdl/proceedings/icpr/2004/2128/03/212830730-abs.html

Al-Ayyoub, M., & Al-Zghool, D. (2013). Determining the type of long bone fractures in x-Ray images. *WSEAS Transactions on Information Science and Applications*, *10*(8), 261–270.

Anu, T., Mallikarjunaswamy, M., of, R. R.-I. J., & 2015, undefined. (n.d.). Detection of bone fracture using image processing methods. *Citeseer*. Retrieved from http://citeseerx.ist.psu.edu/viewdoc/download?doi=10.1.1.739.9543&rep=rep1&type=pdf

Bandyopadhyay, O., … A. B.-C. methods and, & 2016, undefined. (n.d.). Long-bone fracture detection in digital X-ray images based on digital-geometric techniques. *Elsevier*. Retrieved from https://www.sciencedirect.com/science/article/pii/S0169260715002400

Brant, W., & Helms, C. (2012). *Fundamentals of diagnostic radiology*. Retrieved from https://books.google.com.pk/books?hl=en&lr=&id=o_4eoeOinNgC&oi=fnd&pg=PP2&dq=Brant,+William+E+and+Clyde+A+Helms.+Fundamentals+of+Diagnostic+Radiology&ots=mnWcrKw7RA&sig=EW4_XXkvBxMc8pvg7dp45jJ2daA

Bushberg, J., & Boone, J. (2011). *The essential physics of medical imaging*. Retrieved from https://books.google.com.pk/books?hl=en&lr=&id=tqM8IG3f8bsC&oi=fnd&pg=PR1&dq=15.%09Bushberg,+Jerrold+T.+The+Essential+Physics+of+Medical+Imaging.+1st+ed.+Philadelphia:+Lippincott+Williams+%26+Wilkins,+2002.+Print.&ots=9nkx_SjWjo&sig=GP-7jJqIQge8wWZD0u8bnnpaEaY

Chai, H. Y., Wee, L. K., Swee, T. T., Salleh, S., & Ariff, a K. (2011). Gray-Level Co-occurrence Matrix Bone Fracture Detection Center for Biomedical Engineering Biomedical Engineering Group , *8*(1), 26–32. https://doi.org/10.3844/ajassp.2011.26.32

Dhawan, A. P., Huang, H. K., & Kim, D.-S. (2008). *Principles and Advanced Methods in Medical Imaging and Image Analysis*. WORLD SCIENTIFIC. https://doi.org/10.1142/6366

Donnelley, M., & Knowles, G. (2005). where b Y ` b R SUT V c a SUT V qs t r and usv is the

width of the line and, 175–178.

He, J. C., Leow, W. K., & Howe, T. Sen. (n.d.). Hierarchical Classifiers for Detection of Fractures in X-Ray Images. In *Computer Analysis of Images and Patterns* (pp. 962–969). Berlin, Heidelberg: Springer Berlin Heidelberg. https://doi.org/10.1007/978-3-540-74272-2_119

Katherine, A. (2013). *Official CPC Certification Study Guide*. American Medical Association.

Kaur, D., & Kaur, Y. (2014). *International Journal of Computer Science and Mobile Computing Various Image Segmentation Techniques: A Review*. *International Journal of Computer Science and Mobile Computing* (Vol. 3). Retrieved from www.ijcsmc.com

Khurana, J. S. (2009). *Bone pathology*. Humana Press.

Mahendran, S. K., & Baboo, S. S. (2012). Ensemble Systems for Automatic Fracture Detection, *4*(1), 1–4.

Marieb, E. N., & Hoehn, K. (2007). *Human anatomy & physiology*. Pearson Education.

McCance, K. L., & Huether, S. E. (2018). *Pathophysiology-E-Book: The Biologic Basis for Disease in Adults and Children*. Elsevier Health Sciences.

Netter, F. H., Hansen, J. T., & Lambert, D. R. (2005). Netter's clinical anatomy. *2005*, Icon--Learning.

Nixon, M. S., Aguado, A. S., & Elsevier Science Publishers. (2002). *Feature extraction and image processing*. Newnes.

Rizzo, D. C. (2015). *Fundamentals of anatomy and physiology*. Cengage Learning.

Seffinger, M. A., King, H. H., Ward, R. C., Jones, J. M., Rogers, F. J., & Patterson, M. M. (2003). Osteopathic philosophy. *Foundations for Osteopathic Medicine*, *2*, 3–18.

Smith, R., Ward, K., Cockrell, C., Ha, J., & Najarian, K. (2010). DETECTION OF FRACTURE AND QUANTITATIVE ASSESSMENT OF DISPLACEMENT MEASURES IN PELVIC X-RAY IMAGES Dept . Computer Science and VCURES , Virginia Commonwealth University Dept . Emergency Medicine and VCURES , Virginia Commonwealth University. *Emergency Medicine*, 682–685.

Szeliski, R. (2011). *Computer vision : algorithms and applications*. Springer.

Tian, T. P., Chen, Y., Leow, W. K., Hsu, W., Howe, T. Sen, & Png, M. A. (2003). Computing Neck-Shaft Angle of Femur for X-Ray Fracture Detection (pp. 82–89). https://doi.org/10.1007/978-3-540-45179-2_11

Yap, D., Chen, Y., Leow, W., Howe, T., null, M. P.-, & 2004, undefined. (n.d.). Detecting femur fractures by texture analysis of trabeculae. *Computer.Org*. Retrieved from https://www.computer.org/csdl/proceedings/icpr/2004/2128/03/212830730-abs.html